3° Πανελλήνιο Συνέδριο Αντισεισμικής
Μηχανικής & Τεχνικής Σεισμολογίας
5–7 Νοεμβρίου, 2008

Displacement–Based Seismic Design of Structures

G.M. Calvi[1], M.J.N. Priestley[1], and M.J.Kowalsky[2]

[1]IUSS, Pavia, Italy
[2]North Carolina State University, Raleigh, USA

ABSTRACT: The concept of designing structures to achieve a specified performance limit state defined by strain or drift limits was first introduced, in New Zealand, in 1993. Over the following years, and in particular the past five years, an intense coordinated research effort has been underway in Europe and the USA to develop the concept to the stage where it is a viable and logical alternative to current force-based code approaches. Different structural systems including frames, cantilever and coupled walls, dual systems, bridges, wharves, timber structures and seismically isolated structures have been considered in a series of coordinated research programs. Aspects relating to characterization of seismic input for displacement-based design, and to structural representation for design verification using time-history analysis have also received special attention.

This paper summarizes the general design approach, the background research, and some of the more controversial issues identified in a book, currently in press, summarizing the design procedure.

INTRODUCTION

Viewed through the historical prism of the past 100 years, seismic structural design can be seen to have been in constant evolution – much more so than design for other load cases or actions such as gravity, wind, traffic etc. Initially, following structural damage in the seminal earthquakes of the early 20th century (Kanto, Long Beach, Napier), seismic attack was perceived in terms of simple mass-proportional lateral forces, resisted by elastic structural action. In the 1940’s and 50’s the influence of structural period in modifying the intensity of the inertia forces started to be incorporated into structural design, but structural analysis was still based on elastic structural response. Ductility considerations were introduced in the 1960’s and 70’s as a consequence of the experimental and empirical evidence that well-detailed structures could survive levels of ground shaking capable of inducing inertia forces many times larger than those predicted by elastic analysis. Predicted performance came to be assessed by ultimate strength considerations, using force levels reduced from the elastic values by somewhat arbitrary force-reduction factors, that differed markedly between the design codes of different seismically-active countries. Gradually this lead to a further realization, in the 1980’s and 90’s that strength was important, but only in that it helped to reduce displacements or strains, which can be directly related to damage potential, and that the proper definition of structural vulnerability should hence be related to deformations, not strength.

This realization has lead to the development of a large number of alternative seismic design philosophies based more on deformation capacity than strength. These are generally termed “***performance-based”*** design philosophies. The scope of these can vary from comparatively narrow structural design approaches, intended to produce safe structures with uniform risk of damage under specified seismicity levels, to more ambitious approaches that seek to also combine financial data associated with loss-of-usage, repair, and a client-based approach (rather than a code-specified approach) to acceptable risk.

This paper does not attempt to provide such ambitious guidance as implied by the latter approach. In fact, it is our view that such a broad-based probability approach is more appropriate to assessment of designed structures than to the design of new structures. The approach taken in this paper is based on providing the designer with improved tools for ***selecting*** the best structural alternative to satisfy societal (as distinct from client-based) standards for performance, as defined in what we hope will be the next generation of seismic design codes.

The basis of this approach is the procedure termed “**Direct Displacement Based Design”** (**DDBD)**, which was first introduced in 1993 (Priestley, 1993), and has been subjected to considerable research attention, in Europe, New Zealand, and North America in the intervening years. The fundamental philosophy behind **DDBD** is that structures should be designed to achieve a specified performance level, defined by strain or drift limits, under a specified level of seismic intensity. As such, we might describe the designed structures as being “uniform-risk” structures, which would be compatible with the concept of “uniform-risk” spectra, to which we currently design.

The research effort to develop a viable and simple design approach satisfying this goal has considered a wide range of structural types including, frame buildings, wall buildings, dual wall/frame buildings, bridges, seismically isolated structures and wharves, and a range of structural materials, including reinforced and prestressed (precast) concrete, structural steel, masonry and timber. The culmination of this research is a book in press (Priestley et al, 2007) at the time of writing this paper.

The research project behind the design approach, which can now be considered in a rather complete stage of formulation, has had to re-examine a number of long-held basic tenets of earthquake engineering. This re-examination was first presented in 1993, and then updated in 2003. The consequences of this re-examination have been:

- A review of the problems associated with initial-stiffness characterization of structures expected to respond inelastically to the design level of seismicity.
- A review of seismological information to provide more appropriate input for displacement-based design.
- A re-examination of some of the fundamentals of inelastic time-history analysis, particularly aspects related to modelling of elastic damping.
- Development of equations relating equivalent viscous damping to ductility demand for different structural systems.
- Development of alternative methodologies for determining design moments in structural members from design lateral forces.
- A re-examination of capacity-design equations for different structural systems, and development of new, ductility-based equations and methodologies.

The focus throughout this lengthy research project has been on the development of practical and simple seismic design methodology, suitable for incorporation in codes in a format reasonably similar to that currently available for the “Equivalent Lateral Force” approach, but with much improved simulation of structural response. The book summarizing the research includes a chapter containing a draft building code, based entirely on DDBD procedures. It is hoped that this might become a platform for future development of seismic codes. A brief review of items listed above follows.

PROBLEMS WITH SEISMIC DESIGN USING INITIAL STIFFNESS AND SPECIFIED DUCTILITY CAPACITY

Problems with initial-stiffness structural characterization in conventional force-based seismic design, and use of a code-specified ductility capacity have been identified in several previous publications (Priestley 1993, Priestley 2003) and will only be briefly listed in this paper:

- Initial stiffness is not known at the start of the design process, even if member sizes have been selected. This is because the stiffness depends on the strength. Increasing or decreasing reinforcement content to satisfy results of the force-based design proportionally changes the member stiffness. The same conclusion applies to steel members: changing the flange thickness to satisfy a strength requirement changes the member stiffness almost in direct proportion to the strength change.

- Distribution of lateral forces between different parallel structural elements (walls; frames, e.g.) based on elastic estimates of stiffness is illogical and tends to concentrate strength in elements with greatest potential for brittle failure.
- Displacement-equivalence rules relating displacement demand based on initial elastic periods (which are likely, any way, to be significantly in error) to expected inelastic response are invalid, in our view, being based on incorrect elastic damping estimates used in time-history analysis. This is discussed in more detail subsequently.
- Ductility capacity is a function of structural geometry, not just of structural type. Hence it is inappropriate to specify a displacement ductility factor for all structures of the same type (e.g. reinforced concrete frames)
- Seismic design of building structures will generally be governed by drift limits, when realistic estimates of building stiffness are used to determine displacements. Current design approaches require iteration to satisfy drift limits, and codes, such as the NZ concrete code, do not recognize the stiffening effect of added strength unless member sizes are also changed.

DIRECT DISPLACEMENT-BASED SEISMIC DESIGN

The fundamentals of **DDBD** are very simple, and have also been presented in many earlier publications (e.g. Priestley 2000, Priestley, 2003). Only a brief review is included here, with reference to Fig.1 which considers a **SDOF** representation of a frame building (Fig.1(a)), though the basic fundamentals apply to all structural types. The bilinear envelope of the lateral force-displacement response of the **SDOF** representation is shown in Fig.1(b).

While force-based seismic design characterizes a structure in terms of elastic, pre-yield, properties (initial stiffness K_i**,** elastic damping), **DDBD** characterizes the structure by secant stiffness K_e at maximum displacement Δ_d (Fig.1(b)), and a level of equivalent viscous damping ξ**,** representative of the combined elastic damping and the hysteretic energy absorbed during inelastic response. Thus, as shown in Fig.1(c), for a given level of ductility demand, a structural steel frame building with compact members will be assigned a higher level of equivalent viscous damping than a reinforced concrete bridge designed for the same level of ductility demand, as a consequence of "fatter" hysteresis loops.

With the design displacement at maximum response determined as discussed subsequently**,** and the corresponding damping estimated from the expected ductility demand, the effective period T_e at maximum displacement response, measured at the effective height H_e (Fig.1(a)) can be read from a set of displacement spectra for different levels of damping, as shown in the example of Fig.1(d). The effective stiffness K_e of the equivalent **SDOF** system at maximum displacement can be found by inverting the normal equation for the period of a **SDOF** oscillator to provide

$$K_e = 4\pi^2 m_e / T_e^2 \tag{1}$$

where m_e is the effective mass of the structure participating in the fundamental mode of vibration. From Fig.1(b), the design lateral force, which is also the design base shear force is thus

$$F = V_{Base} = K_e \Delta_d \tag{2}$$

The design concept is thus very simple. Such complexity that exists relates to determination of the characteristics of the equivalent **SDOF** structure, the determination of the design displacement, and development of design displacement spectra.

Design Displacement

The characteristic design displacement of the substitute structure depends on the limit state displacement or drift of the most critical member of the real structure, and an assumed displacement shape for the structure. This displacement shape is that which corresponds to the inelastic first-mode at the design level of seismic excitation. Thus the changes to the elastic first-mode shape resulting from local changes to member stiffness caused by inelastic action in plastic hinges are taken into account at the beginning of the design. Representing the displacement by the inelastic rather than the elastic first-mode shape is consistent with characterizing the structure by its secant stiffness to maximum response. In fact, the inelastic and elastic first-mode shapes are often very similar.

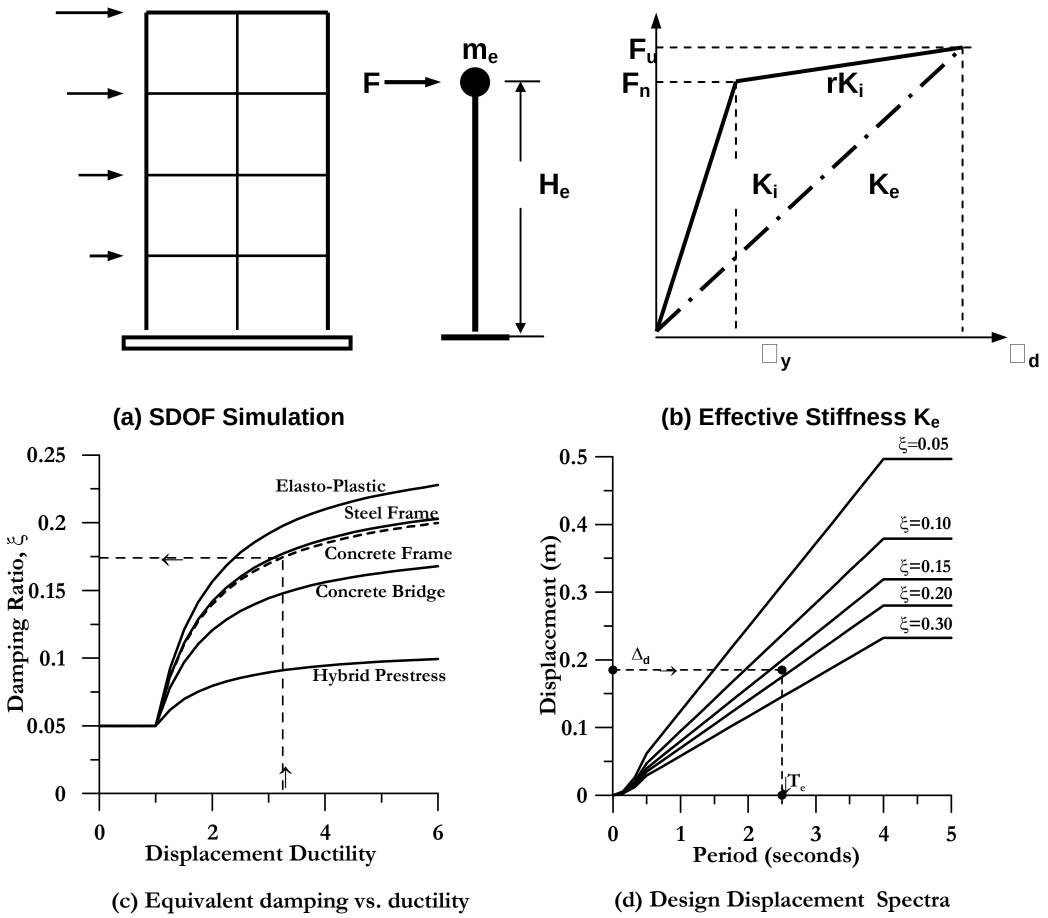

Fig.1 Fundamentals of DDBD

The design displacement of the equivalent **SDOF** structure (the generalized displacement coordinate) is thus given by

$$\Delta_d = \sum_{i=1}^{n}\left(m_i\Delta_i^2\right) / \sum_{i=1}^{n}\left(m_i\Delta_i\right) \tag{3}$$

where m_i and Δ_i are the masses and displacements of the n significant mass locations respectively. For multi-storey buildings, these will normally be at the n floors of the building. For bridges, the mass locations will normally be at the centre of the mass of the superstructure above each column, but the superstructure mass may be discretized to more than one mass per span to improve validity of simulation. With tall columns, such as may occur in deep valley crossings, the column may also be discretized into multiple elements and masses.

Where strain limits govern, the design displacement of the critical member can be determined by integration of the curvatures corresponding to the limit strains. Similar conclusions apply when code drift limits apply. For example, the design displacement for frame buildings will normally be governed by drift limits in the lower storeys of the building. For a bridge, the design displacement will normally be governed by the plastic rotation capacity of the shortest column. With a knowledge of the displacement of the critical element and the design displacement shape, the displacements of the individual masses are given by

$$\Delta_i = \delta_i \cdot \left(\frac{\Delta_c}{\delta_c} \right) \qquad (4)$$

where δ_i is the inelastic mode shape, and Δ_c is the design displacement at the critical mass, ***c***, and δ_c is the value of the mode shape at mass ***c***. Specific details on structural mode shapes for **DDBD** of different structural types are given in the book (Priestley et al 2007).

Note that the influence of higher modes on the displacement and drift envelopes are generally small, and are not considered at this stage in the design. However, for buildings higher than (say) ten storeys, dynamic amplification of drift may be important, and the design drift limit may need to be reduced to account for this. This factor is considered in detail in the relevant structural design chapters.

Effective Mass

From consideration of the mass participating in the first inelastic mode of vibration, the effective system mass for the substitute structure is

$$m_e = \sum_{i=1}^{n} \left(m_i \Delta_i \right) / \Delta_d \qquad (5)$$

where Δ_d is the design displacement given by Eq.(3). Typically, the effective mass will range from about 70% of the total mass for multi-storey cantilever walls to more than 85% for frame buildings of more than 20 storeys. For simple multi-span bridges the effective mass will often exceed 95% of the total mass. The remainder of the mass participates in the higher modes of vibration. Although modal combination rules, such as the *square-root-sum-of-squares* (**SRSS**) or *complete quadratic combination* (**CQC)** rules may indicate a significant increase in the elastic base shear force over that from the first inelastic mode, there is much less influence on the design base overturning moment. The effects of higher modes are inadequately represented by elastic analyses and are better accommodated in the capacity design phase, rather than the preliminary phase of design.

Structure Ductility Demand

Determination of the appropriate level of equivalent viscous damping requires that the structural ductility be known. This is straightforward since the design displacement has already been determined, and the yield displacement depends only on geometry, not on strength. Relationships for yield curvature of structural elements, such as walls, columns, beams etc have been established (Priestley 2003) in the general form:

$$\phi_y = C_1 \varepsilon_y / h \qquad (6)$$

where C_1 is a constant dependent on the type of element considered, ε_y is the yield strain of the flexural reinforcement and ***h*** is the section depth. Yield drifts for concrete and steel frames can be expressed as

$$\theta_y = C_2 \varepsilon_y \frac{L_b}{h_b} \tag{7}$$

where L_b and h_b are the beam span and depth, respectively, and C_2 = 0.5 and 0.65 for concrete and structural steel respectively. For building structures, equations (6) and (7) can readily be integrated to obtain the displacement at the effective height, H_e, given by

$$H_e = \sum_{i=1}^{n}(m_i \Delta_i H_i) / \sum_{i=1}^{n}(m_i \Delta_i) \tag{8}$$

where H_i are the heights of the n storeys.

The displacement ductility demand for the structures is thus known at the start of the design, by Eq.(9), even though the strength is not yet established:

$$\mu = \Delta_d / \Delta_y \tag{9}$$

From relationships between structural type, ductility demand, and equivalent viscous damping, discussed in the following section, the appropriate level of elastic damping to use in Fig.1(d) can be directly obtained, and hence the base shear force calculated (Eq.(2)). This base shear force is then distributed to the structural masses in accordance with Eq.(10), and the structure analysed, as also discussed subsequently.

$$F_i = V_{Base}(m_i \Delta_i) / \sum_{i=1}^{n}(m_i \Delta_i) \tag{10}$$

EQUIVALENT VISCOUS DAMPING

A key element of **DDBD** is that hysteretic damping is modelled by equivalent viscous damping (**EVD)**, using relationships such as those presented in Fig.1(c). The total equivalent damping is the sum of elastic, ξ_{el} and hysteretic, ξ_{hyst} damping:

$$\xi_{eq} = \xi_{el} + \xi_{hyst} \tag{11}$$

Both components need some examination.

Hysteretic component

The approach adopted has been to use values of **EVD** that have been calibrated for different hysteresis rules (see Fig.2, for examples) to give the same peak displacements as the hysteretic response, using inelastic time-history analysis. Two independent studies, based on different methodologies were used to derive the levels of equivalent viscous damping. The first involved the use of a large number of real earthquake accelerograms (Dwairi and Kowalsky, 2006), where the equivalent viscous damping was calculated for each record, ductility level, effective period and hysteresis rule separately, and then averaged over the records to provide a relationship for a given rule, ductility, and period. The second study (Grant et al, 2005), using a wider range of hysteresis rules was based on a smaller number of spectrum-compatible artificial accelerograms where the results of the elastic and inelastic analyses were separately averaged, and compared. In each case the equivalent viscous damping was varied until the elastic results of the equivalent substitute structure matched that of the real hysteretic model.

The two studies initially were carried out without additional elastic damping, for reasons that will become apparent in the following section. It was found that the approaches resulted in remarkably similar relationships for equivalent viscous damping for all hysteresis rules except elastic-perfectly plastic (**EPP**), where the discrepancy was about 20%. It is felt that the difference for the **EPP** rule is a consequence of the use of real records, with comparatively short durations of strong ground motion in the first study, and artificial records, with longer strong ground motion durations in the second study. **EPP** hysteresis is known to be sensitive to duration effects.

Elastic component

Elastic damping is used in inelastic time-history analysis to represent damping not captured by the hysteretic model adopted for the analysis. This may be from the combination of a number of factors, of which the most important is the typical simplifying assumption in the hysteretic model of perfectly linear response in the elastic range (which therefore does not model damping associated with the actual elastic non-linearity and hysteresis). Additional damping also results from foundation compliance, foundation non-linearity and radiation damping, and additional damping from interaction between structural and non-structural elements.

The damping coefficient, and hence the damping force depends on what value of stiffness is adopted. In most inelastic analyses, this has been taken as the initial stiffness. This, however, results in large and spurious damping forces when the response is inelastic, which, it has been argued in a previous NZSEE conference (Priestley et al 2005) is inappropriate, and that tangent stiffness should be used as the basis for elastic damping calculations. With tangent stiffness, the damping coefficient is proportionately changed every time the stiffness changes, associated with yield, unloading or reloading, etc. This results in a reduction in damping force as the structural stiffness softens following yield, and a reduction in the energy absorbed by the elastic damping. Since the hysteretic rules are invariably calibrated to model the full structural energy dissipation subsequent to onset of yielding, this approach to characterization of the elastic damping is clearly more appropriate than is initial-stiffness elastic damping. The significance to structural response of using tangent-stiffness rather than initial-stiffness damping has been discussed in detail in Priestley et al (2005) and Priestley et al (2007). However, in **DDBD**, the initial elastic damping ratio adopted in Eq.(11) is related to the secant stiffness to maximum displacement, whereas it is normal in inelastic time-history analysis to relate the elastic damping to the initial (elastic) stiffness, or more correctly, as noted above, to a stiffness that varies as the structural stiffness degrades with inelastic action (tangent stiffness). Since the response velocities of the “real” and “substitute” structures are expected to be similar under seismic response, the damping forces of the “real” and “substitute” structures, which are proportional to the product of the stiffness and the velocity will differ significantly, since the effective stiffness k_e of the substitute structure is approximately equal to $k_{eff} = k_i/$□ (for low post-yield stiffness). Priestley and Grant (2005) has determined the adjustment that would be needed to the value of the elastic damping assumed in DDBD (based on either initial-stiffness or tangent-stiffness proportional damping) to ensure compatibility between the “real” and “substitute” structures. Without such an adjustment, the verification of DDBD by inelastic time-history analysis would be based on incompatible assumptions of elastic damping.

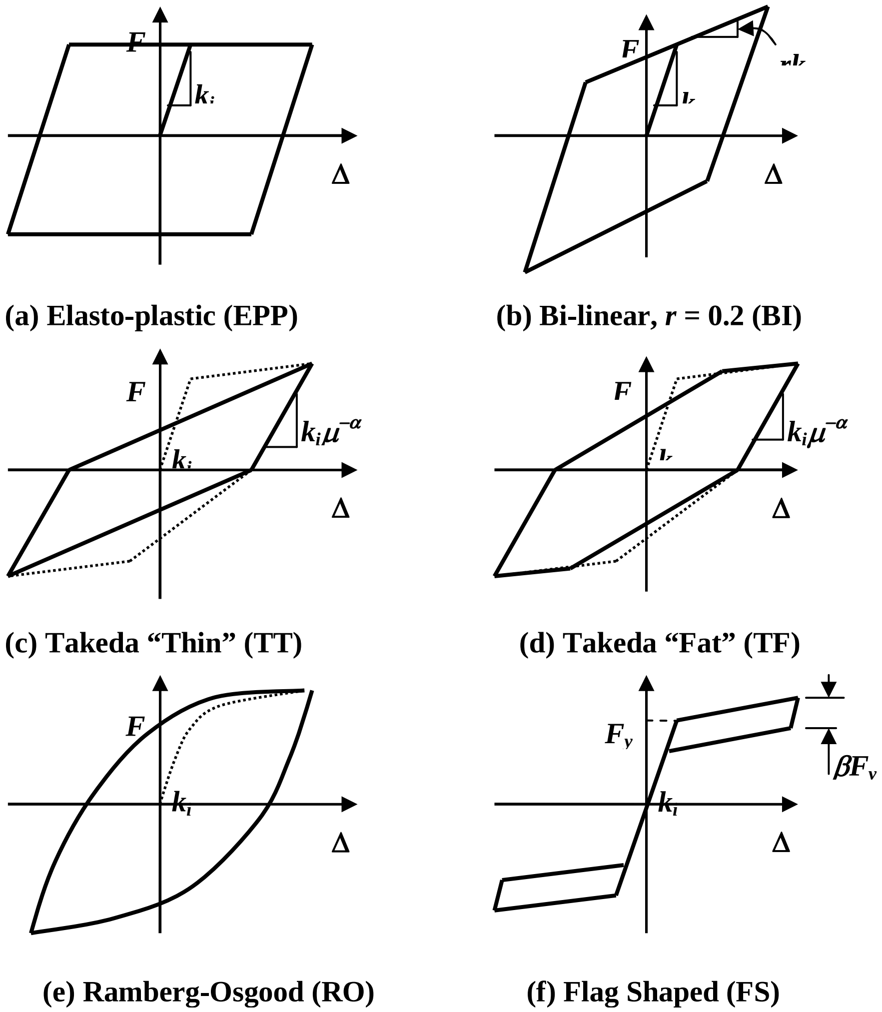

Fig.2 Hysteresis Rules Considered in Time-History Analyses

The adjustments depend on whether initial-stiffness damping (conventional practice), or tangent-stiffness damping (correct procedure, we believe) is adopted for time-history analysis. If initial-stiffness damping is chosen, the elastic damping coefficient used in **DDBD** must be larger than the specified initial-stiffness damping coefficient; if tangent-stiffness is chosen, it must be less than the specified tangent-stiffness coefficient. It is possible to generate analytical relationships between the substitute-structure and "real" structure elastic damping coefficients that are correct for steady-state harmonic response. However, as with the hysteretic component, these are not appropriate for transient response to earthquake accelerograms, though the trends from time-history response follow the form of the theoretical predictions. Hence, to obtain the appropriate correction factors, it is again necessary to rely on the results of inelastic time-history analyses. Priestley and Grant (2005) compared results of elastic substitute-structure analyses with inelastic time history results to determine the correction factor to be applied to the elastic damping coefficient for the assumptions of either initial-stiffness or tangent-stiffness elastic damping. The form of Eq.(11) is thus slightly changed to:

$$\xi_{eq} = \kappa\xi_{el} + \xi_{hyst} \tag{12}$$

The correction factor κ is plotted for different hysteresis rules, and for different initial damping assumptions (initial-stiffness or tangent-stiffness) in Fig.3. It is possible to include the ductility dependency of the elastic damping inside the basic form of the equivalent viscous damping equations. With the usual assumption of 5% elastic damping, the damping –ductility relationships can be expressed in the general form:

$$\xi_{eq} = 0.05 + C_3\left(\frac{\mu - 1}{\mu\pi}\right) \qquad (13)$$

where the coefficient C_3 varies between 0.1 and 0.7 (for the assumption of tangent-stiffness elastic damping) depending on the hysteresis rule appropriate for the structure under design (Priestley et al (2007)).

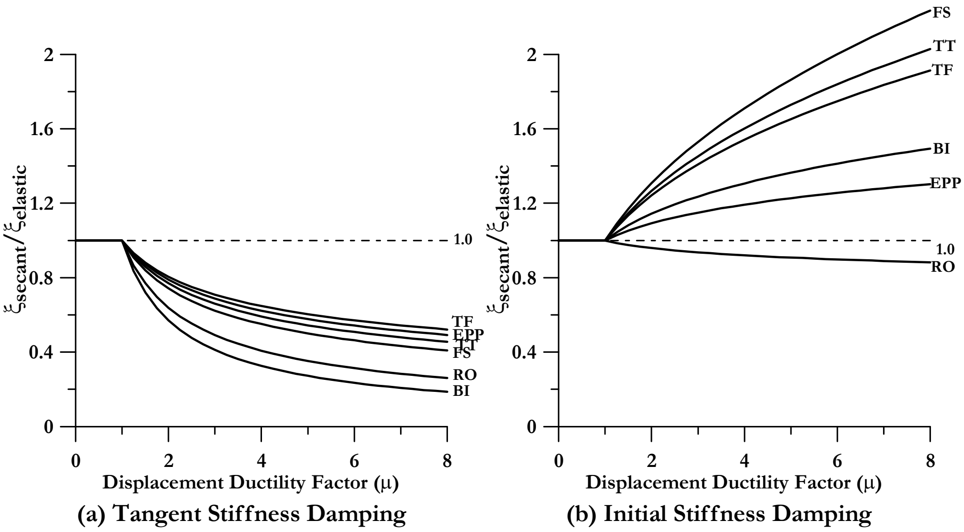

Fig.3 Secant Stiffness Equivalent Elastic Viscous Damping Related to Initial Elastic Stiffness and Elastic Damping Model

Damping in Mixed Systems

In conventional force-based design there is some difficulty in assessing the appropriate level of ductility to use in determining required base-shear strength for mixed systems, such as wall/frames, or even wall structures with walls of different length in a given direction. In **DDBD** the procedure is straightforward, with the **EVD** of the different structural lateral-force-resisting elements being separately calculated and then combined, weighted by the proportion of base-shear force (or overturning moment) carried. Details are presented in the Priestley et al (2007).

ANALYSIS UNDER LATERAL FORCES

Two alternative methods of structural analysis under the design vector of lateral forces represented by Eq.(10) are suggested as appropriate for **DDBD.** Each is briefly described here, with reference to frame buildings.

Stiffness-Based Analysis

Conventional force-based design would analyse the structure using estimates of elastic member stiffness. As already discussed, these stiffness estimates are likely to be significantly in error, since the stiffness depends on the strength, which is not at this stage known. For **DDBD** we examine analysis procedures with reference to the simple four-storey frame of Fig.4. To be consistent with the principles of **DDBD,** the frame structure analysed should represent the relative stiffness of members at the peak displacement. Thus beams, which are expected to sustain ductility demands should have their stiffnesses reduced from the elastic cracked-section stiffness in proportion to the expected member displacement ductility demand. For frame members of normal proportions, it will be adequate to reduce the elastic stiffness of all beam members by the system displacement ductility level □□. An improved solution will result if the member ductilities at different levels are proportional to the drift demands (assuming that the beams at different levels have constant depth). Thus the member ductility at the first floor beams will be taken as 1.33□□**,** and at the roof level, as 0.667□□.

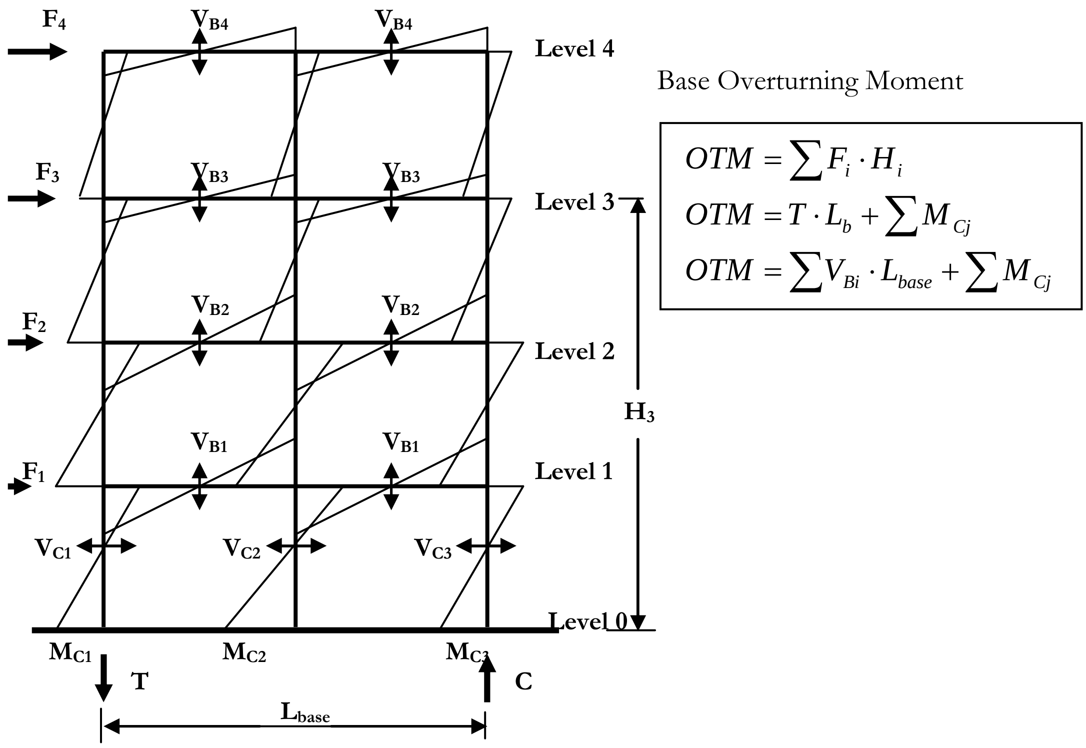

Fig.4 Seismic Moments from DDBD Lateral Forces

The design philosophy of weak beams/strong columns will require that the columns between the first floor and the roof remain essentially elastic. Hence, the stiffness of these columns should be modelled by the cracked-section stiffness, without any reduction for ductility.

A problem occurs with the structural characterization of the columns between the ground and first floors. The design philosophy requires that plastic hinges be permitted to form at the ground floor level to complete the desired beam-sway mechanism, but that the first-storey columns remain elastic at the first floor level, to ensure that a soft-storey (column sway) mechanism of inelastic displacement cannot develop. It is thus not clear how the stiffness of the ground floor columns should be represented in the structural analysis.

The solution to this problem relies on the recognition that any structural analysis is approximate (compare the relative structural approximations involved in an initial-stiffness and a secant-stiffness representation, both of which are valid at different levels of seismic response), and that the fundamental requirement is that equilibrium is maintained between internal and external forces. With this in mind, we realise that it is possible for the designer to select the moment capacities of the column-base hinges, provided that the resulting moments throughout the structure are in equilibrium with the applied forces. Since our design criterion is that column hinges do not form at the underside of the level 1 beams, it would appear logical to design in such a way that the point of contraflexure in the columns occurs approximately at 60% of the storey height. The design moment at the column base will thus be $0.6\boldsymbol{V_C H_1}$ where $\boldsymbol{V_C}$ is the column shear and $\boldsymbol{H_1}$ is the first-storey height. This implies that the maximum column moment at the base of the first floor beam under first-mode response is about 0.325$\boldsymbol{V_C}$, or about 54% of the column-base moment capacity. We note that the column shear can be directly determined from the lateral forces, provided logical decisions are made about the distribution of storey shears between columns. Thus, with reference to the four-storey frame of Fig.4, the total base shear of

$$V_{Base} = F_1 + F_2 + F_3 + F_4 = V_{C1} + V_{C2} + V_{C3} \qquad (14)$$

should be distributed between the columns in proportion to the beam moment input. If we design for equal positive and negative moment capacity of the beams at a given level, then the moment input from the beams to the central column will be twice that for the exterior columns. The corresponding distribution of the base shear between the columns will thus be

$$V_{C2} = 2V_{C1} = 2V_{C3} = 0.5V_{Base} \qquad (15)$$

The desired column-base moment capacities can then be defined before the structural analysis for required flexural strength of beam plastic hinges. The structural analysis then proceeds with the first-storey columns modelled as having cracked-section stiffness, and pinned-base conditions. The base moments (e.g. $\boldsymbol{M_1}$ = 0.6$\boldsymbol{V_{C1}H_1}$) are then applied as forces to the column-base hinges, in addition to the applied lateral forces $\boldsymbol{F_1}$ to $\boldsymbol{F_4}$.

Equilibrium-Based Analysis

A problem with the stiffness-based analysis described in the previous section is that, as with force-based design, the member stiffness values are not known until the strength is allocated. Although the use of stiffness values reduced by ductility demand, and of defined base-moments reduces the sensitivity to assumptions of relative stiffness, a more satisfying, and simpler approach to the structural analysis can be obtained purely from equilibrium considerations.

Beam Moments

We again refer to the regular frame of Fig.4, and consider equilibrium at the foundation level. The lateral seismic forces induce column-base moments, and axial forces in the columns. The total overturning moment (***OTM***) induced by the lateral forces at the base of the building is

$$OTM = \sum_{i=1}^{n} F_i H_i = \sum_{j=1}^{m} M_{cj} + T.L_{base} \qquad (16)$$

where $\boldsymbol{M_{Cj}}$ are the column base moments (***m*** columns) ***T = C*** are the seismic axial forces in the exterior columns, and $\boldsymbol{L_{base}}$ is the distance between ***T*** and ***C***. The tension force ***T*** (and the compression force ***C***) is the sum of the beam shear forces, $\boldsymbol{V_{Bi}}$ up the building:

$$T = \sum_{i=1}^{n} V_{Bi} \qquad (17)$$

Equations (15) to (17) can be combined to find the required sum of the beam shears in a bay:

$$\sum_{i=1}^{n} V_{Bi} = T = \left(\sum_{i=1}^{n} F_i H_i - \sum_{j=1}^{m} M_{Cj} \right) / L_{base} \qquad (18)$$

Any distribution of total beam shear force up the building that satisfies Eq.(18) will result in a statically admissible equilibrium solution for the **DDBD**. Thus as with the choice of column-base moment capacity, it is also to some extent a designer's choice how the total beam shear force is distributed. However, it has been found, from inelastic time-history analyses that drift is controlled best by allocating the total beam shear from Eq.(18) to the beams in proportion to the storey shears in the level below the beam under consideration. This can be expressed as

$$V_{Bi} = T \cdot \frac{V_{S,i}}{\sum_{i=1}^{n} V_{S,i}} \tag{19}$$

Seismic beam moments can now be determined from the beam shears from the relationship

$$M_{Bi,l} + M_{Bi,r} = V_{Bi} \cdot L_{Bi} \tag{20}$$

where L_{Bi} is the beam span between column centrelines, and $M_{Bi,l}$ and $M_{Bi,r}$ are the beam moments at the column centrelines at the left and right end of the beam, respectively. The relative proportions of the moments at each end can be chosen to reflect the influence of slab reinforcement, and gravity moments, if so desired.

Column moments

Column base moments will be determined in the same fashion as in the previous section. Column design moments at other elevations can then be determined from statics, knowing the column shears in each storey, and the moment input to the joint centroids from the beam moments. Since the column moments will be amplified by capacity design principles, the exact magnitude is not required.

CAPACITY DESIGN PROTECTION IN DDBD

The concept of capacity design was developed in New Zealand by Dr. John Hollings, and Profs. Tom Paulay and Bob Park. Although it is fair to say that New Zealand still leads the world in codified capacity design provisions, there is room for re-examination, particularly as related to **DDBD**. The coordinated research project outlined at the start of this paper has had particular emphasis on examining existing, and developing new capacity design rules and procedures for a range of different structural types, including framed buildings, structural wall buildings, dual wall/frame buildings, bridges, and marginal wharves.

The general requirement for capacity protection can be defined by Eq.(21):

$$\phi_S S_D \geq S_R = \phi^o \omega S_E \tag{21}$$

where S_E is the value of the design action being capacity protected, corresponding to the design lateral force distribution found from the **DDBD** process, ϕ^o is the ratio of overstrength moment capacity to required capacity of the plastic hinges, ω is the amplification of the action being considered, due to higher mode effects, S_D is the design strength of the capacity protected action, and ϕ_S is a strength-reduction factor relating the dependable and design strengths of the action.

In **DDBD** the design strength of plastic hinges is based on conservative but realistic estimates of material strengths, including strain hardening and concrete confinement, where appropriate, and is matched to the demand at maximum displacement. No strength reduction factor is used for **DDBD**. As a consequence, the overstrength factor ϕ^o to be used in design is significantly lower than with current design.

On the other hand, it has been clear for some time that a significant omission in NZ capacity design rules is the lack of a ductility modifier. Time-history analyses clearly show that higher mode effects are closely related to ductility demand. Modal superposition approaches, where the higher-mode actions as well as the actions in the fundamental mode are divided by the ductility or force-reduction factor can be seriously non-conservative, particularly for structures braced with walls. The same statement can be made about existing simplified approaches following the general form of Eq.(21). Comparative results are shown in Figs.5 and 6 for moment and shear envelopes of multi-storey walls, excited by different multiples (between 0.5 and 2) of the design intensity (Priestley and Amaris, 2001). In these plots **IR** indicates design intensity, and a value of **IR** = 1.5 indicates an excitation of 1.5 times the design intensity. Also indicated in the plots by dashed lines are capacity design envelopes corresponding to NZ code provisions (indicated as **Cap.Des)** and modal superposition, where the elastic modal responses have been combined by the **SSRS** combination rule and divided by the design ductility factor (indicated as **SSRS**/□).

Two points are immediately apparent from these plots. First, the current capacity design envelopes are generally non-conservative at the design intensity. Second, the non-conservatism increases as the intensity increases, clearly indicating a dependency on displacement ductility demand, since this increases as the intensity increases. The excess demand over capacity is particularly worrying for shear strength.

A basic and simple modification to the modal superposition method (termed *modified modal superposition* (**MMS**) herein) is available by recognizing that ductility primarily acts to limit first-mode response, but has comparatively little effect in modifying the response in higher modes. If this were to in fact be the case, then first-mode response would be independent of intensity, provided that the intensity was sufficient to develop the base moment capacity, while higher modes would be directly proportional to intensity. This approach is very similar to that proposed by Eibl and Keintzel (1988) as a means for predicting shear demand at the base of cantilever walls.

In this approach, shear force profiles were calculated based on the following assumptions.

- First-mode shear force was equal to the shear profile corresponding to development of the base moment capacity, using the displacement-based design force vector. However, for low seismic intensity, where plastic hinging was not anticipated in the wall, simple elastic first mode response, in accordance with the elastic response spectrum was assumed.
- Higher-mode response was based on elastic response to the acceleration spectrum appropriate to the level of seismic intensity assumed, using the elastic higher-mode periods. Force-reduction factors were not applied.
- The basic equation to determine the shear profile was thus:

$$V_{MMS,i} = \left(V_{1D,i}^2 + V_{2E,i}^2 + V_{3E,i}^2 + \ldots\right)^{0.5} \qquad (22)$$

where $V_{MMS,i}$ is the shear at level i, $V_{1D,i}$ is the lesser of elastic first mode, or ductile (**DDBD** value) first-mode response at level i, and V_{2Ei}, and V_{3Ei} etc are the elastic modal shears at level i for modes 2, 3 etc. Predictions based on this approach are compared with average time-history results in Fig.7. Agreement is very close, though the **MMS** approach tends to become increasing conservative at high intensity levels (i.e. high ductility levels), particularly for taller walls. A similar approach for predicting moments in structural walls was equally successful.

It has been found that improved predictions can be obtained when the modal analysis is based on a structural model where the member stiffness is reduced to the secant level appropriate at maximum design displacement. Although the effect is minor for wall structures, it is a significant improvement for frames and bridges.

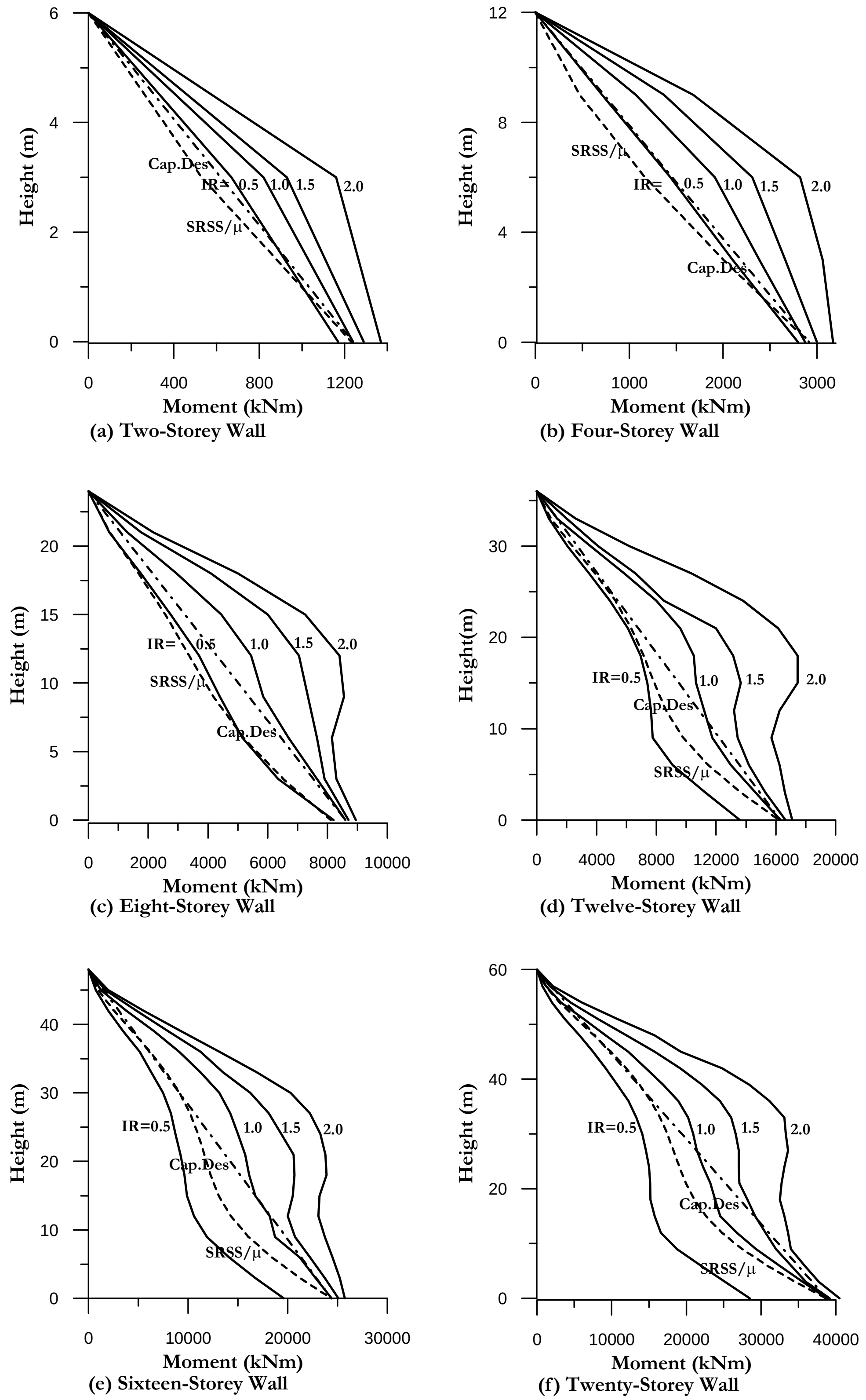

Fig.5 Comparison of Capacity Design Moment Envelopes with Results of Time-History Analyses for Different Seismic Intensity Ratios

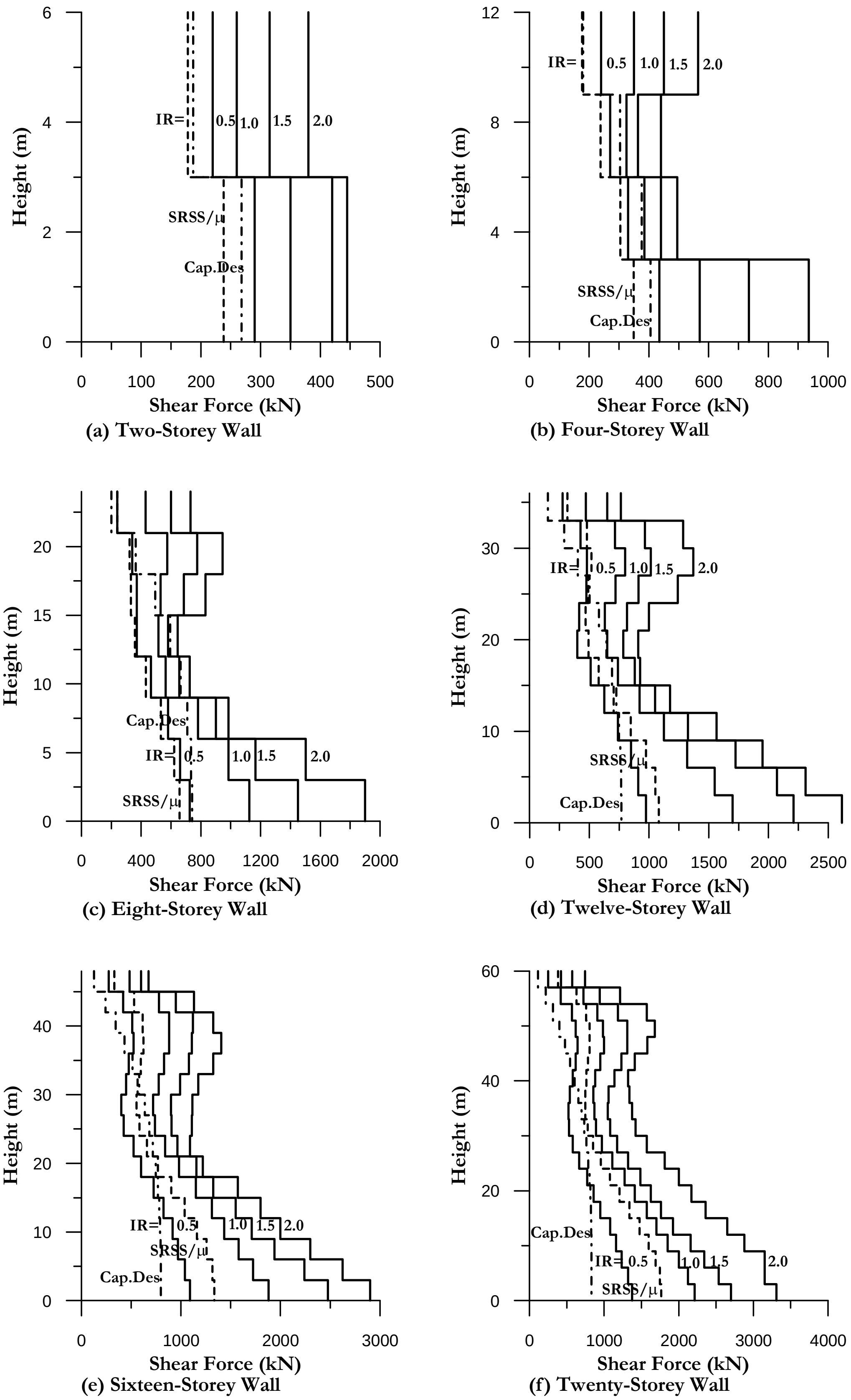

Fig.6 Comparison of Capacity Design Shear Force Envelopes with Results of Time-History Analyses for Different Seismic Intensity Ratios

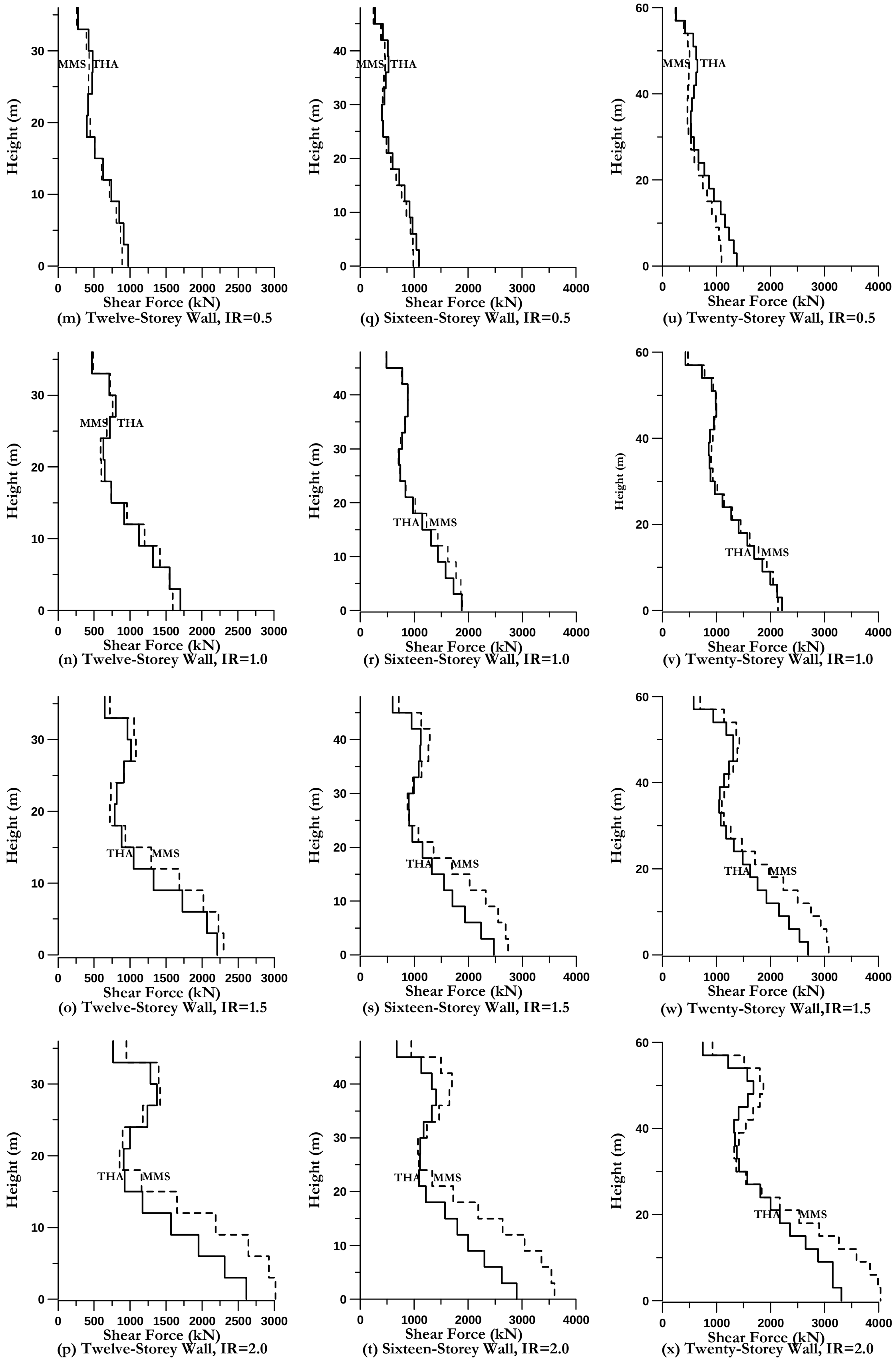

Fig.7 Comparison of Modified Modal Superposition (MMS) Shear Force Envelopes with Time-History Results, for Different Seismic Intensities

Simplified Capacity Design

In many cases the additional analytical effort required to carry out modal analysis of the designed wall structure to determine the capacity design distribution of moments and shears will be unwarranted, and a simpler, conservative approach, similar to existing capacity design rules may be preferred. As part of the research effort into **DDBD**, simplified rules have been developed for frames, walls, wall/frames and bridges.

As an example, we continue with the case of cantilever wall structures.

Moment Capacity Design Envelope for Cantilever Walls

A bi-linear envelope is defined by the overstrength base moment capacity $\phi^o M_{Base}$, the mid-height overstrength moment demand $M^o_{0.5H}$, and zero moment at the wall top, as illustrated in Fig.8(a) for a four-storey wall. The overstrength base moment is determined from section and reinforcement properties using moment-curvature analysis, or using simplified prescriptive overstrength factors, guidance for which is given in Priestley et al (2007). The mid-height moment is related to the overstrength base moment by the equation:

$$M^o_{0.5Hn} = C_{1,T} \cdot \phi^o M_{Base} \qquad (23a)$$

where

$$C_{1,T} = 0.4 + 0.075T_i\left(\frac{\mu}{\phi^o} - 1\right) \geq 0.4 \qquad (23b)$$

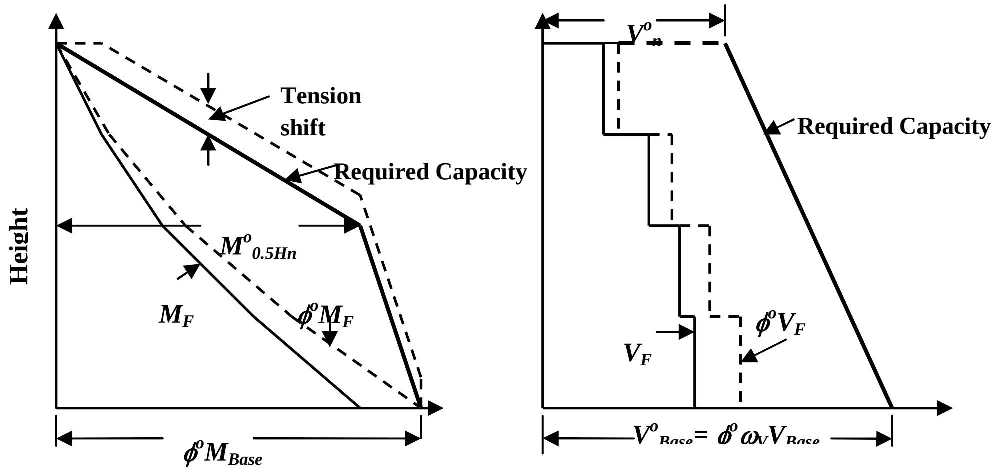

(a) Moment Capacity Envelope **(b) Shear Force Capacity Envelope**

Fig. 8 Simplified Capacity Design Envelopes for Cantilever Walls

In Eq.(23b), T_i is the initial (elastic) cracked-section period of the structure. Note that μ/ϕ^o is the effective displacement ductility factor at overstrength, and that tension shift effects should be considered when terminating flexural reinforcement.

1.1.1 *Shear Capacity Design Envelopes for Cantilever Walls*

The shear force capacity-design envelope is defined by a straight line between the base and top of the wall, as indicated in Fig.8(b). The design base shear force is defined by:

$$V^o_{Base} = \phi^o \omega_V V_{Base}, \qquad (24a)$$

where $$\omega_V = 1 + \frac{\mu}{\phi^o} C_{2,T} \tag{24b}$$

and $$C_{2,T} = 0.067 + 0.4(T_i - 0.5) \leq 1.15 \tag{24c}$$

The design shear force at the top of the wall, V^o_n is related to the shear at the bottom of the wall by:

$$V_n^o = C_3 V_{Base}^o \tag{25a}$$

where $$C_3 = 0.9 - 0.3T_i \geq 0.3 \tag{25b}$$

Predictions for the ratio of wall moment at mid-height to base moment, and dynamic amplification factor for base shear force are compared with values obtained in the **ITHA** for different elastic periods and ductility levels in Fig.9.

Similar simplified capacity-design equations are presented for different structural systems.

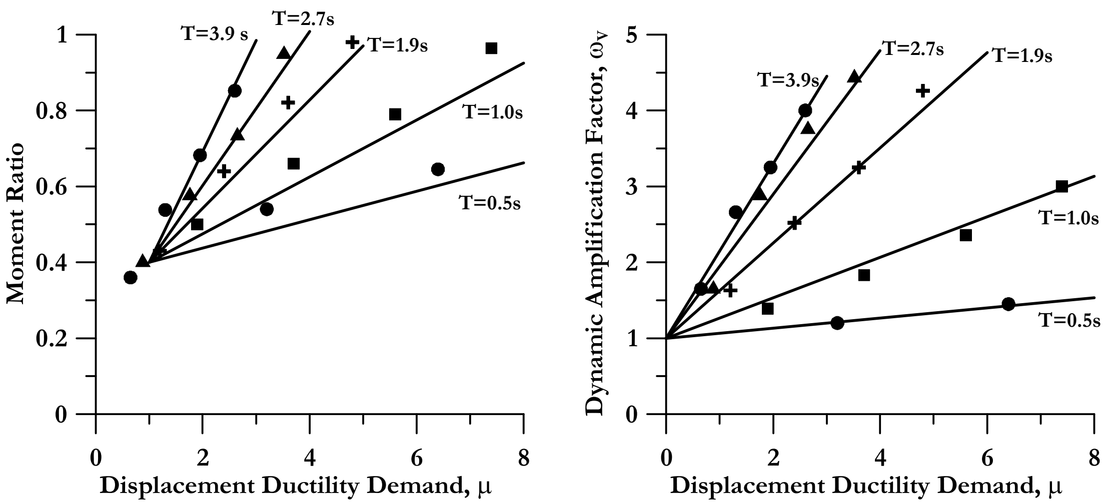

Fig.9 Comparison of Capacity Design Equations (24) and (25) with Time History Results for Different Elastic Periods and Ductility Levels

SEISMIC INPUT FOR DDBD

As is apparent from Fig.1(d), the displacement response spectrum is used rather than an acceleration spectrum to determine the required base shear strength. It is possible to generate the displacement spectrum from existing acceleration response spectra, assuming steady-state sinusoidal response, but this assumption becomes increasingly inaccurate at long periods. It should be noted that this inaccuracy has been cited as a criticism of displacement-based design, since **DDBD** uses the effective period at maximum displacement response, which is approximately √□ times the elastic period used for force-based design, where response is presumably better known. This criticism does not stand up to scrutiny, however, since the elastically designed structure will respond inelastically with the same period as used for design of an equivalent **DDBD** structure, and hence any uncertainty in the long period response data will be reflected in inaccuracies in the displacement-equivalence rule (such as equal-displacement) used to relate elastic to inelastic displacements in force-based design.

Recently considerable research attention has been focused by seismologists on improving the accuracy of displacement design spectra. The approach tentatively adopted in Priestley et al (2007) is developed from recent work by Faccioli et al (2004), who analysed a large number of recent high-quality digital accelerograms. These indicated that design elastic response displacement spectra could be reasonably represented as linear up to a displacement plateau initiating at a corner period $\boldsymbol{T_C}$, the value of which depends on the moment magnitude, $\boldsymbol{M_w}$. For $\boldsymbol{M_w} > 5.7$:

$$T_c = 1.0 + 2.5\left(M_w - 5.7\right)\text{sec} \tag{26}$$

with a corresponding displacement amplitude for 5% damping of

$$\delta_{\max} = C_S \cdot \frac{10^{(M_W - 3.2)}}{r}\ \text{mm} \tag{27}$$

where $\boldsymbol{r}$ is the epicentral distance (or nearest distance to the fault plane for large earthquakes) in km, and where $\boldsymbol{C_S}$ =1.0 for firm ground. The response displacements resulting from Eq.(2.5) should be modified for other than firm ground. Tentative suggestions are as follows:

Rock: $\boldsymbol{C_S} = 0.7$
Firm Ground: $\boldsymbol{C_S} = 1.0$
Intermediate Soil: $\boldsymbol{C_S} = 1.4$
Very soft Soil: $\boldsymbol{C_S} = 1.8$

Predictions based on Eqs.(26) and (27) with $\boldsymbol{C_S} = 1.0$ are plotted in Fig.10 for different $\boldsymbol{M_w}$ and $\boldsymbol{r}$.

Recent unpublished work by Faccioli indicates that it is probable that the corner period and corresponding plateau displacement will be revised upwards by about 20%. It should be noted that there are unresolved differences in predictions of corner period between US seismologists (based mainly on seismological theory) and European seismologists (mainly empirically based).

Displacement-based seismic design using a secant stiffness representation of structural response requires a modification to the elastic displacement response spectrum to account for ductile response. The influence of ductility can be represented either by equivalent viscous damping (as shown in Fig.1(d) or directly by inelastic displacement spectra for different ductility levels. The use of spectra modified by different levels of damping requires relationships between ductility and damping to be developed for different structural hysteretic characteristics as discussed in Section 4 above, but enables a single design spectrum to be used for all structures. The use of spectra modified by different levels of ductility is perhaps more direct, but requires the ductility modifiers to be determined for each hysteretic rule considered. The same inelastic time-history analyses can be used to develop both approaches, which are essentially identical.

A commonly used expression for relating the displacement response spectrum for a damping ratio of □ to the elastic spectrum for □ = 0.05 was presented in the 1998 edition of Eurocode EC8 (EC8 1998), and is shown below in Eq.(28):

$$R_\xi = \left(\frac{0.07}{0.02 + \xi}\right)^{0.5} \tag{28}$$

Although a more recent edition of EC8 (EC8 2003) revised the coefficients of numerator and denominator of Eq.(28) to 0.10 and 0.05 respectively, our analyses of real and artificial records convince us that the form given in Eq.(28) gives a better representation of the damped spectra.

Equation (28) applies to sites where forward directivity effects are not apparent. It would also be desirable to have an equivalent expression for sites where forward directivity velocity pulse characteristics might be expected. It has been suggested (Priestley 2003) based on limited data, that a modification to the 1998 EC8 expression given by

$$R_\xi = \left(\frac{0.07}{0.02 + \xi} \right)^{0.25} \tag{29}$$

might be appropriate. Some qualified support for Eq.(29) is available in Bommer and Mendis (2005) which provides additional discussion of this topic.

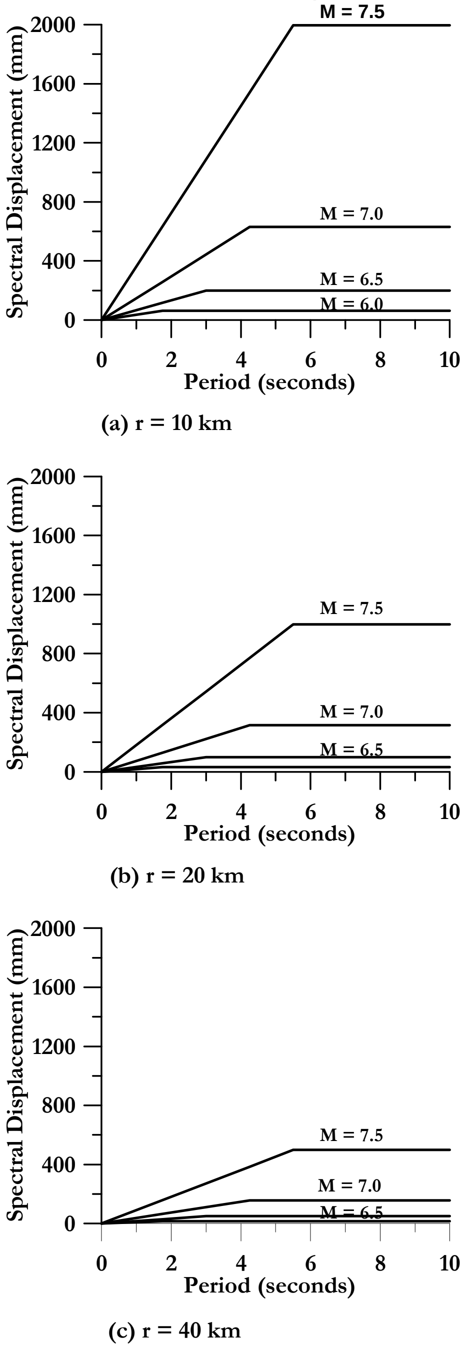

Fig.10 Influence of Magnitude and Distance on 5% Damped Displacement Spectra for Firm Ground Using Eqs.(24) and (25) [after Faccioli et al (2005)]

BRIEF NOTES ON OTHER DDBD ISSUES

Space limitations do not allow adequate coverage of the many additional aspects covered in

Priestley et al (2007). Brief notes on some of the more controversial issues are included in this section.

Torsion in DDBD

Paulay (2001) and Castillo and Paulay (2004) have shown that elastic analysis based on initial- stiffness structural representation is inadequate to predict inelastic torsional response. This work has been extended in the present study to develop a design methodology for **DDBD** of structures with torsional eccentricity. Design displacement of the centre of mass is reduced by a torsional component which can be estimated with some accuracy at the start of the design process. The approach combines stiffness and strength eccentricity, and uses the effective stiffness of lateral force-resisting elements at maximum displacement response. Thus for seismic attack parallel to a principal axis of a building the structural elements parallel to the direction of attack have their elastic stiffness reduced by the design ductility factor, while the orthogonal elements are assigned their elastic (cracked-section) stiffness. The method provides accurate estimates of both centre-of-mass displacements, and displacements of structural elements with maximum torsional components of displacement, for both torsionally unrestrained (TU) and torsionally restrained (TR) systems, as indicated in Fig.11.

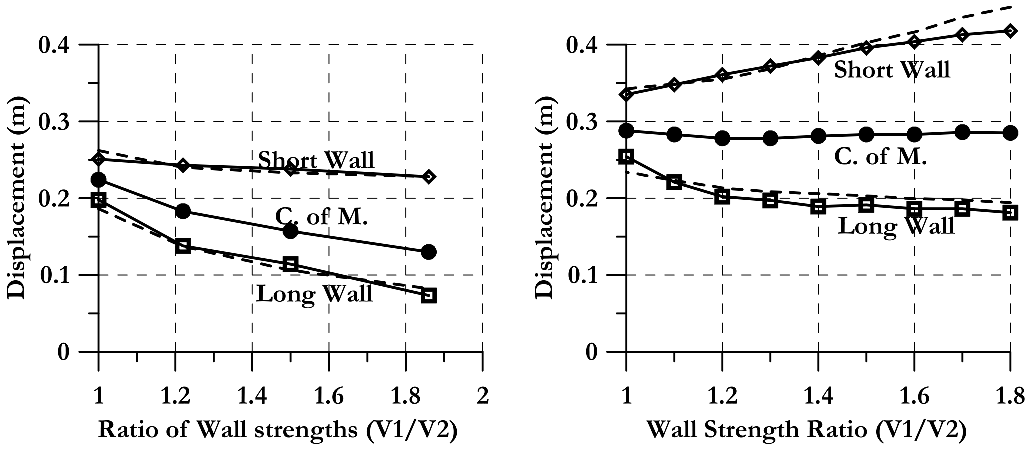

(a) TU system, system strength increases (Castillo and Paulay 2004 data)

(b) TR system, constant strength (Beyer 2007 data)

Fig.11 Comparison between Predicted Displacements (dashed lines) and Average Time-History Results (solid lines and data points) for TU and TR systems

1.2 P-δ Effects in DDBD

The treatment of **P-δ** effects in **DDBD** is comparatively straightforward, and is illustrated in Fig. 12(c). Unlike conditions for force-based design, the design displacement is known at the start of the design process, and hence the **P-δ** moment is also known before the required strength is determined. **DDBD** is based on the effective stiffness at maximum design displacement. When **P-δ** moments are significant, it is the stiffness corresponding to the degraded strength and the design displacement (see K_e in Fig.12(c)) that must match the required stiffness. Hence, Eq.(2) defines the required residual strength. The initial strength, corresponding to zero displacement, is thus given by

$$F = K_e \Delta_d + C \cdot \frac{P\Delta_d}{H} \tag{30}$$

and hence the required base-moment capacity is

$$M_B = K_e \Delta_d H + C \cdot P\Delta_d \tag{31}$$

Note that it is more consistent to define the **P-δ** effect in terms of the base moment, than the equivalent lateral force. In Eq.(31), for consistency with the design philosophy of **DDBD**, we should take ***C***=1. However, examination of the hysteretic loops indicates that more energy will be absorbed, for a given final design displacement and degraded strength, than for a design when **P-δ** design is not required, particularly for concrete-like response. It is also apparent from time-history analyses that for small values of the stability index, displacements are only slightly increased when **P-δ** moments are ignored, as noted above. It is also clear that steel structures are likely to be more critically affected than will concrete structures. Consideration of these points leads to the specification of ***C*** =1 for steel structures and ***C*** =0.5 for concrete structures. Recent time-history analyses (Pettinger and Priestley 2007) have provided confirmation of these recommendations.

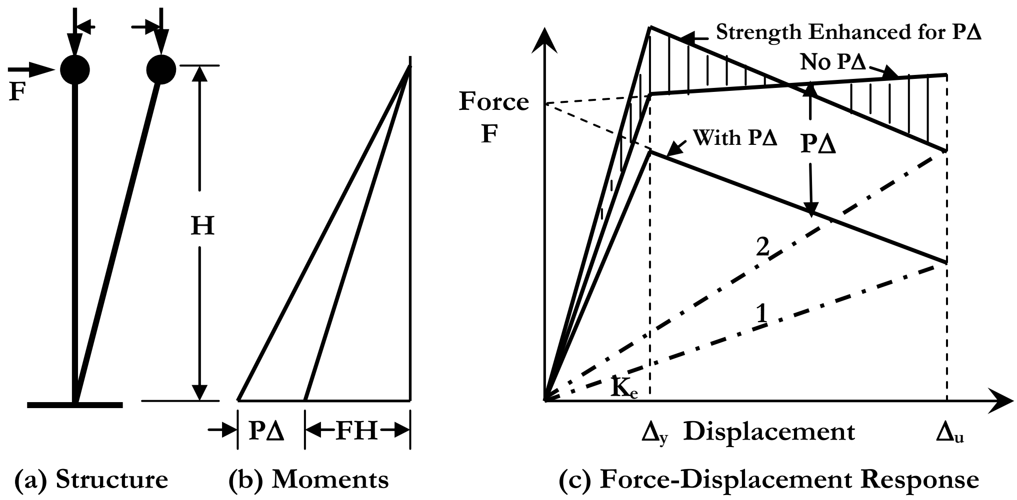

Fig.12 P-δ Effects on Design Moments

Combination of Gravity and Seismic Forces in DDBD

When gravity moments are added to seismic moments in potential plastic hinge regions to result in a total design moment that exceeds the seismic moments, then the consequence is a reduction in the ductility demand below the level selected for design. In **DDBD** the consequence would be a response displacement less than the selected design displacement. It is argued in Priestley et al (2007) that it is illogical to directly add gravity and seismic moments when different effective stiffness is implied in the analyses for the two effects. For example, in a frame building, at maximum response plastic hinges will have formed at the beam ends, greatly reducing the stiffness of the end regions. An elastic analysis of the gravity load moments in the beam taking account of this reduction in stiffness of the end regions would indicate a very substantial decrease in the fixed end moments, and an increase in the mid-span moment from the value applying with elastic beam properties. This is, of course, a justification for moment-redistribution.

Comparative analyses (Pinto 1997) of frames where the fixed-end moments from gravity loads were alternatively included or neglected have shown that the displacement response of frames was essentially unaffected. This result together with the above comments lead us to recommend that plastic hinge regions of structures be designed for the larger of moments resulting from factored gravity loads or from seismic forces, but not combined gravity and seismic moments. This simplifies design, and for many structures is very similar, but more conservative than the common gravity+seismic+30% redistribution approach, as illustrated for a typical frame design in Fig.13.

Draft DDBD Building Code

In order to show how **DDBD** philosophy might be incorporated into a code document, the relative provisions have been organised in one chapter of Priestley et al (2007) into a code plus commentary type format that could act as the basis for development of an alternative **DDBD** code for seismic design of buildings. With minor modification it could also apply to other structures such as bridges, seismic isolated structures, unreinforced masonry structures and wharves, all of which are considered in the book.

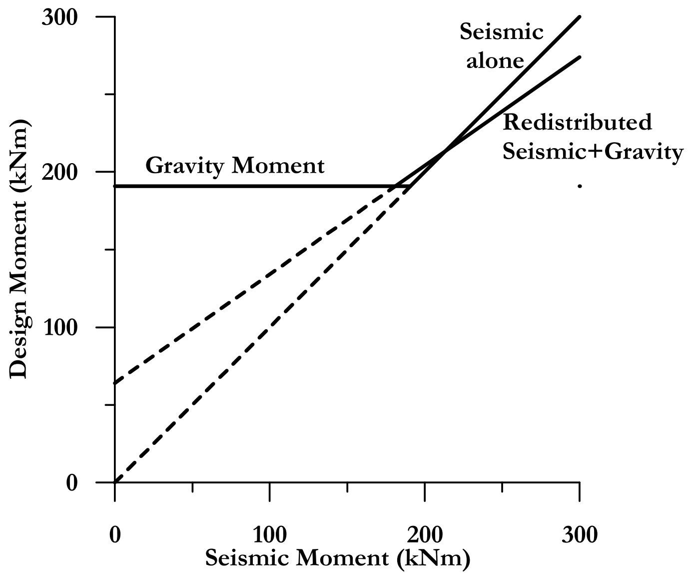

Fig.13 Typical Frame Design Moments Based on Maximum of Factored Gravity or Seismic Compared with Combined and Redistributed Moments

CONCLUSIONS

The major coordinated research project described in this paper presents an alternative approach to current force-based design. Although it may appear controversial in many of its recommendations, it is based on sound engineering principles, and, we believe is much more rational than current seismic design methodology. Above all, it is simple to apply in the design office once a few basic concepts have been grasped.

The state of development of the approach is now rather mature, with detailed consideration of “real” engineering issues, such as MDOF systems, torsional response, irregularity of structural layout, P-□ effects, and a wide range of different structural types including walls, frames, dual systems, bridges and seismic isolated structures. Materials considered include reinforced, prestressed, and precast concrete, structural steel, masonry and timber. The approach has also been developed as an assessment tool for existing structures to complement the design approach. A very large number of MDOF structures of a wide range of structural type and material have been subjected to inelastic-time-history analysis to verify the accuracy of displacement predictions, and to provide the necessary data base to develop the extensive, and new, capacity design provisions. A list of the chapter headings in Priestley et al (2007) is included in an Appendix to this paper. Extensive design examples are also included in this reference.

REFERENCES

Beyer K., Displacement-Based Design of Torsionally Eccentric Structures" (2007) *PhD Thesis, European School for Advanced Studies in Reduction of Seismic Risk" Pavia* (in preparation)

Bommer, J.J. and Mendis, R. (2005) "Scaling of Spectral Displacement Ordinates with Damping Ratios". *Earthquake Engg. and Str. Dyn. 34:* pp 145-165

Castillo, R. (2004) "Seismic Design of Asymmetric Ductile Systems", PhD Thesis, University of Canterbury, Christchurch, New Zealand (Paulay supervisor)

Eibl, J. and Keintzel, F. (1988) "Seismic Shear Forces in RC Cantilever Shear Walls". *Proceedings, 9th World Conference on Earthquake Engineering, Paper 9-1-1,* Tokyo/Kyoto*.*

EC8 (1998) "Design Provisions for Earthquake Resistance of Structures" *Pub. ENV-1998-2, Comite Europeaen de Normalization, Brussels*

EC8 (2003) "Design Provisions for Earthquake Resistance of Structures" *Pub. ENV-2003-2, Comite Europeaen de Normalization, Brussels*

Faccioli, E., Paolucci, R., and Rey, J. (2004) Displacement Spectra for Long Periods. *Earthquake Spectra,* Vol 10(2) pp347-376

Dwairi, H.M, Kowalsky, M.J. and Nau, J.M. (2006) "Equivalent Viscous Damping in Support of Direct Displacement-Based Design" *Journal of Earthquake Engineering*

Paulay, T. (2001) "Some Design Principles Relevant to Torsional Phenomena in Ductile Buildings" *Journal of Earthquake Engineering"* Vol.5, No.3 pp 273-308

Pettinger, J.D., and Priestley, M.J.N. (2007) "Direct Displacement-Based Seismic design Including P-Effects" *European School for Advanced Studies in Reduction of Seismic Risk, Research Report* (in Preparation)

Pinto, P. (Ed). (1997) "Seismic Design of Concrete Structures, for controlled inelastic response " CEB Bulletin N.236, ,*Comité Euro-International du Béton Lausanne*, ISSN 0378-9489

Priestley, M.J.N. (1993) "Myths and Fallacies in Earthquake Engineering – Conflicts Between Design and Reality" *Bulletin, NZSEE* 26(3), pp329-341

Priestley, M.J.N. (2000) "Performance-Based Seismic Design" *Keynote Address, Proc. 12th World Conference on Earthquake Engineering"* Auckland 22pp

Priestley, M.J.N. and Amaris A.D. (2002) "Dynamic Amplification of Seismic Moments and Shear Forces in Cantilever Walls" *European School for Advanced Studies in Reduction of Seismic Risk, Research Report ROSE-2002/01*, 95 pages

Priestley, M.J.N. (2003) Myths and Fallacies in Earthquake Engineering, Revisited. *The Mallet Milne Lecture, 2003, IUSS Press, Pavia*, 121 pp*.*

Priestley, M.J.N. and Grant, D.N. (2005) Viscous Damping in Seismic Design and Analysis *Journal of Earthquake Engineering Vol 9 Special Issue* pp 229-255

Priestley, M.J.N., Grant, D.N., and Blandon, C.(2005) "Direct Displacement-Based Seismic Design" *Proc. NZSEE Annual Conference.*

Priestley M.J.N., Calvi, M.C., and Kowalsky, M.J. (2007) Displacement-Based Seismic Design of Structures *IUSS Press,* Pavia, , 670 pp.